Photonics-Based Single Sideband Mixer With Ultra-High Carrier and Sideband Suppression

Chongjia Huang and Erwin H. W. Chan, *Senior Member, IEEE*

***Abstract*—A photonics-based frequency mixer for up converting an IF signal into an RF signal with very large suppression in the carrier and the sideband is presented. The mixer is filter free and has a simple structure. It enables off-the-shelf bias controllers to be incorporated into the system. This solves the problem of the carrier and sideband suppression reduces with time that is present in all reported photonics-based single sideband mixers. Experiments are conducted to verify the proposed mixer structure. Results show the single sideband mixer generates an up converted RF signal with more than 40 dB suppression in the carrier and sideband over a wide frequency range. This is a 10-dB improvement compared to the reported structures. A conversion efficiency of around -6 dB is attained, which is over 10 dB higher than the reported structures. Frequency up conversion of an IF signal with a band of frequency and a long-term stable performance are also demonstrated.**

***Index Terms*—Optical fibre communication, optical signal processing, optical modulators, frequency conversion, microwave mixer.**

I. Introduction

FREQUENCY mixer is a key component in radars, instruments and communication systems. It either up converts a low-frequency IF signal into a high-frequency RF signal or down converts a high-frequency RF signal into a low-frequency IF signal. Realising microwave frequency mixing operation in the optical domain has the benefits of wide bandwidth, high isolation and electromagnetic interference immunity compared to the traditional electronic frequency mixers. It also has the potential to reduce the system size and cost via eliminating an external electrical LO source [1]. Hence, numerous microwave photonic mixer structures have been reported [2]–[14]. Among them, only few are focused on single sideband (SSB) mixing [9]–[14]. A SSB mixer is used for up converting an IF signal with a frequency of f_{IF} into an RF signal at the frequency of either f_{LO}+f_{IF} or f_{LO}-f_{IF} where f_{LO} is the frequency of the LO into the mixer. It reduces the system cost and complexity by eliminating the need of using a filter to remove one sideband. It also improves the spectrum efficiency [12].

Sideband and carrier suppression are important parameters in SSB mixers. They are defined as the ratio of the RF signal power to the undesired sideband and carrier power at the mixer output. Table I summarises the configuration and the performance of the reported photonics-based SSB mixers. This shows most reported photonics-based SSB mixers can achieve around 30 dB sideband and carrier suppression, which is higher than the 23-dB suppression obtained using a commercial 6-18 GHz SSB mixer (Marki Microwave SSB-0618) but is lower than the 36-dB suppression obtained in a commercial 0.8-2.5 GHz SSB mixer (Analog Devices AD8346). Conversion efficiency, which is defined as the ratio of the output RF signal power to the input IF signal power, is another important mixer parameter. Table I shows the conversion efficiency of the reported photonics-based SSB mixers is less than -16 dB. It is a challenge to implement a SSB mixer with a wide bandwidth, a larger carrier and sideband suppression and a high conversion efficiency.

In this paper, we present a photonics-based SSB mixer that largely improves both the carrier and sideband suppression and the conversion efficiency of the reported structures. It is filter free and has a simple single-laser, single-integrated-modulator and single-photodetector structure. The problem of drift in the modulator operating point that reduces the carrier and sideband suppression in photonics-based SSB mixers was pointed out in [10] but until now it has not been solved. The proposed structure enables bias controllers to be incorporated into the system to eliminate the modulator bias drift problem. The performance of the proposed SSB mixer is analysed. The requirements to obtain an over 40 dB sideband and carrier suppression are discussed. Experimental results are presented which demonstrate wideband SSB frequency mixing operation with around 10 dB improvement in both the carrier and sideband suppression and the conversion efficiency compared to the reported structures. SSB frequency up conversion of a 200 Mbps pseudo random binary sequence (PRBS) signal with around 40 dB carrier and sideband suppression and a long-term stable performance obtained using bias controllers in the setup are also demonstrated.

II. Topology and Operation Principle

Fig. 1 shows the structure of the proposed microwave photonic SSB mixer. It mainly consists of a laser, an electro-optic modulator and a photodetector (PD). The electro-optic modulator used to implement the SSB mixer is a dual-polarisation dual-drive Mach Zehnder modulator (DPol-DDMZM). The modulator is formed by a 3-dB coupler, two dual-drive MZMs ($\mathrm{DDMZM_X}$ and $\mathrm{DDMZM_Y}$), a polarisation rotator (PR) and a polarisation beam combiner (PBC). Each dual-drive MZM has two RF ports for microwave signal modulation and a DC port for setting

Manuscript received May 11, 2021; revised June 10, 2021; accepted June 11, 2021. Date of publication June 15, 2021; date of current version July 1, 2021. *(Corresponding author: Erwin H. W. Chan.)*

The authors are with the College of Engineering, IT and Environment, Charles Darwin University, Darwin, NT 0909, Australia (e-mail: 1286660746@qq.com; erwin.chan@cdu.edu.au).

Digital Object Identifier 10.1109/JPHOT.2021.3089575

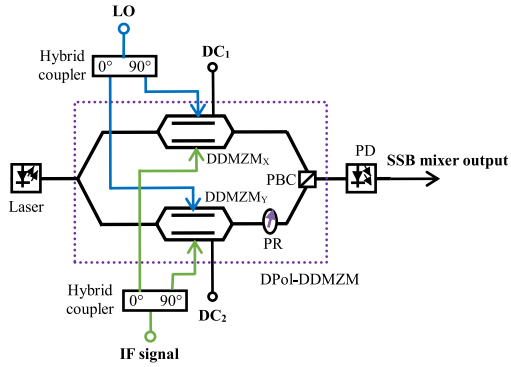

Fig. 1. Structure of the proposed microwave photonic SSB mixer.

the modulator bias point. Both $\mathrm{DDMZM_X}$ and $\mathrm{DDMZM_Y}$ are biased at the minimum transmission point. The IF signal, which needs to be up converted into a high-frequency RF signal, is split into two by a 90° hybrid coupler. An LO, which is a single frequency tone, is also split into two by another 90° hybrid coupler. As shown in Fig. 1, $\mathrm{DDMZM_X}$ is driven by a 90° phase shifted LO and an IF signal. Since a dual-drive MZM can be modelled as two optical phase modulators connected in parallel, the electric field at $\mathrm{DDMZM_X}$ output is the sum of the LO and IF phase modulated optical signals, which can be expressed as

$$E_X(t) = \frac{1}{2\sqrt{2}} E_{in}\sqrt{t_{ff}}e^{j\omega_c t} \left[e^{jm_{LO}\sin\left(\omega_{LO}t+\pi/2\right)} + e^{j(m_{IF}\sin(\omega_{IF}t)+\pi)}\right] \quad (1)$$

where E_{in} is the electric field amplitude of the continuous wave light into the DPol-DDMZM, t_{ff} is the dual-drive MZM insertion loss, $\omega_c = 2\pi f_c$, $\omega_{LO} = 2\pi f_{LO}$ and $\omega_{\mathrm{IF}} = 2\pi f_{IF}$ are the angular frequency of the continuous wave light, the LO and the IF signal respectively, $m_{LO(IF)} = \pi V_{LO(IF)}/V_{\pi,RF}$ is the LO (IF signal) modulation index, $V_{LO(IF)}$ is the voltage of the LO (IF signal) into the RF port of the dual-drive MZM and $V_{\pi,RF}$ is the dual-drive MZM RF port half-wave voltage. Using the Jacobi-Anger expansion, (1) can be written as

$$E_X(t) = \frac{1}{2\sqrt{2}} E_{in}\sqrt{t_{ff}}e^{j\omega_c t} \begin{bmatrix} J_0(m_{LO}) + jJ_1(m_{LO})e^{j\omega_{LO}t} + jJ_1(m_{LO})e^{-j\omega_{LO}t} \\ -J_0(m_{IF}) - J_1(m_{IF})e^{j\omega_{IF}t} + J_1(m_{IF})e^{-j\omega_{IF}t} \\ -J_2(m_{IF})e^{j2\omega_{IF}t} - J_2(m_{IF})e^{-j2\omega_{IF}t} \\ -J_3(m_{IF})e^{j3\omega_{IF}t} + J_3(m_{IF})e^{-j3\omega_{IF}t} \end{bmatrix} \quad (2)$$

where $J_n(x)$ is the nth order Bessel function of the first kind. Note that the second and higher order LO sidebands are neglected in (2) as the frequency components generated by these sidebands after photodetection are far away from the desired output RF signal frequency. The fourth and higher order IF signal sidebands are also neglected in (2) as they have small amplitudes. The electric field at $\mathrm{DDMZM_Y}$ output can be obtained using the same technique described above and is written as

$$E_Y(t) = \frac{1}{2\sqrt{2}} E_{in}\sqrt{t_{ff}}e^{j\omega_c t} \begin{bmatrix} J_0(m_{LO}) + J_1(m_{LO})e^{j\omega_{LO}t} - J_1(m_{LO})e^{-j\omega_{LO}t} \\ -J_0(m_{IF}) - jJ_1(m_{IF})e^{j\omega_{IF}t} - jJ_1(m_{IF})e^{-j\omega_{IF}t} \\ +J_2(m_{IF})e^{j2\omega_{IF}t} + J_2(m_{IF})e^{-j2\omega_{IF}t} \\ +jJ_3(m_{IF})e^{j3\omega_{IF}t} + jJ_3(m_{IF})e^{-j3\omega_{IF}t} \end{bmatrix} \quad (3)$$

(2) and (3) show the amplitude and phase of different optical frequency components at the two dual-drive MZM outputs. It is important to note that the polarisation state of the optical signal at the output of $\mathrm{DDMZM_Y}$ is rotated by 90° via a PR. Therefore, the optical frequency components produced by $\mathrm{DDMZM_X}$ and $\mathrm{DDMZM_Y}$ at the DPol-DDMZM output have an orthogonal polarisation state. They do not interact with each other at the PD. Beating of the optical frequency components produced by the individual dual-drive MZM at the PD generates the RF signal at f_{LO}+f_{IF} together with unwanted frequency components. The SSB mixer output photocurrent is given by

$$I(t) = \Re\left(E_X \cdot {E_X}^* + E_Y \cdot {E_Y}^*\right) \quad (4)$$

where $\Re$ is the PD responsivity and $*$ denotes complex conjugate. Under an ideal situation, no carriers at f_{LO} is present at the SSB mixer output because the carriers generated by the LO sidebands at f_c±f_{LO} beat with the optical carrier at f_c have an opposite phase and hence they cancel each other. The generation of the RF signal at f_{LO}+f_{IF} and the sideband at f_{LO}-f_{IF} can be seen from $\mathrm{DDMZM_X}$ and $\mathrm{DDMZM_Y}$ output optical spectrums shown in Fig. 2. The solid double-arrow lines in the figures show beating of the LO and IF signal sidebands at the PD, which produces the RF signal at f_{LO}+f_{IF}. The dashed double-arrow lines show beating of the LO and IF signal sidebands at the PD, which produces the unwanted sideband at f_{LO}-f_{IF}. Fig. 2(a) and 2(b) show the sideband at f_{LO}-f_{IF} generated by the two dual-drive MZMs are out of phase and hence they cancel each other. On the other hand, the two RF signals at f_{LO}+f_{IF} are in phase. Therefore, the SSB mixer output electrical spectrum contains the sum of these two RF signals. Using the technique described above, it was found that the intermodulation products at f_{LO}±2f_{IF} and f_{LO}+3f_{IF} are eliminated in the same manner as the sideband at f_{LO}-f_{IF}. The intermodulation product at f_{LO}-3f_{IF} is the only unwanted frequency component present at the SSB mixer output under an ideal situation. The photocurrent in (4) can be written as

$$I(t) = \frac{1}{4}\Re P_{in} t_{ff} J_1(m_{LO})\left[-J_1(m_{IF})\sin\left(\left(\omega_{LO}+\omega_{IF}\right)t\right) + J_3(m_{IF})\sin\left(\left(\omega_{LO}-3\omega_{IF}\right)t\right)\right] \quad (5)$$

where P_{in} is the power of the continuous wave light into the DPol-DDMZM. The ratio of the output RF signal power to the power of the intermodulation product at f_{LO}-3f_{IF} is above 48.5 dB for an IF signal modulation index of below 0.3. Note from Fig. 2 that the proposed microwave photonic SSB mixer output optical spectrum consists of two pairs of sidebands with an optical carrier being suppressed. This is the same as the

TABLE I
REPORTED AND PROPOSED PHOTONICS-BASED SSB FREQUENCY MIXER CONFIGURATION WITH MEASURED CARRIER AND SIDEBAND SUPPRESSION AND CONVERSION EFFICIENCY. DPMZM: DUAL-PARALLEL MACH ZEHNDER MODULATOR; OBPF: OPTICAL BANDPASS FILTER; DP-DPMZM: DUAL-POLARISATION DUAL-PARALLEL MACH ZEHNDER MODULATOR; DPOL-DDMZM: DUAL-POLARISATION DUAL-DRIVE MACH ZEHNDER MODULATOR

Reference	Configuration	Suppression	Conversion efficiency	Output optical power
[9]	DPMZM	23 dB	-25.7 dB	6.5 dBm
[10]	DPMZM with OBPF	30 dB	-18.2 dB	5 dBm
[11]	DP-DPMZM with OBPF	30 dB	-16.3 dB	-
[12]	DPMZM	30 dB	-	-
[13]	DPol-DDMZM with OBPF	30 dB	-	-
[14]	DPMZM with OBPF	30 dB	-	5 dBm
Current work	DPol-DDMZM	40 dB	-6 dB	10 dBm

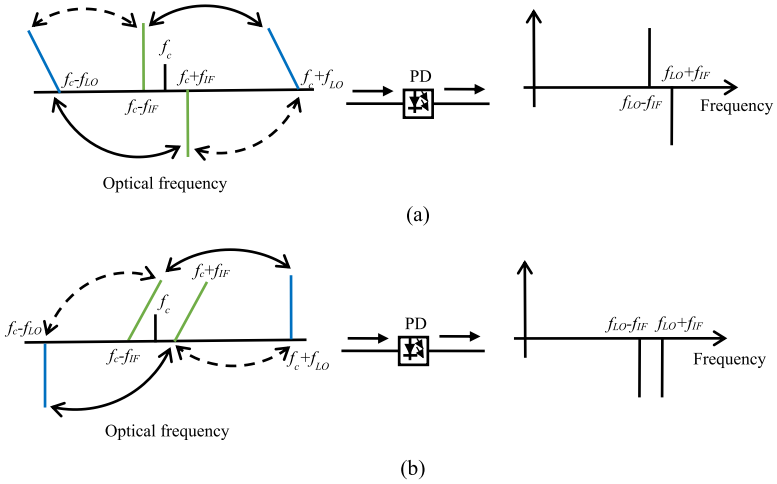

Fig. 2. Optical spectrum showing the optical carrier and the first order LO and IF signal sidebands generated by (a) $\mathrm{DDMZM_X}$ and (b) $\mathrm{DDMZM_Y}$, and the RF signal and sideband at the PD output. f_c, f_{LO} and f_{IF} are the frequency of the optical carrier, the LO and the IF signal respectively.

conventional dual-parallel modulator based microwave photonic mixer [5]. A high conversion efficiency can be obtained by using an LO modulation index that is slightly larger than the IF signal modulation index.

In practice, a carrier, sideband and intermodulation products are present at the SSB mixer output. This is because 90° hybrid couplers have amplitude and phase imbalance, and electro-optic modulators have the bias drift problem. With the inclusion of these non-ideal effects, the electric field at the output of $\mathrm{DDMZM_X}$ and $\mathrm{DDMZM_Y}$ can be written as

$$E_X(t) = \frac{1}{2\sqrt{2}} E_{in} \sqrt{t_{ff}} e^{j\omega_c t} \begin{bmatrix} J_0(\alpha_{LO} m_{LO}) + jJ_1(\alpha_{LO} m_{LO}) e^{j(\omega_{LO} t + \theta_{LO})} \\ +jJ_1(\alpha_{LO} m_{LO}) e^{-j(\omega_{LO} t + \theta_{LO})} \\ -J_0(m_{IF}) e^{j\beta_X} - J_1(m_{IF}) e^{j(\omega_{IF} t + \beta_X)} \\ +J_1(m_{IF}) e^{-j(\omega_{IF} t - \beta_X)} - J_2(m_{IF}) e^{j(2\omega_{IF} t + \beta_X)} \\ -J_2(m_{IF}) e^{-j(2\omega_{IF} t - \beta_X)} - J_3(m_{IF}) e^{j(3\omega_{IF} t + \beta_X)} \\ +J_3(m_{IF}) e^{-j(3\omega_{IF} t - \beta_X)} \end{bmatrix} \quad (6)$$

$$E_Y(t) = \frac{1}{2\sqrt{2}} E_{in} \sqrt{t_{ff}} e^{j\omega_c t} \begin{bmatrix} J_0(m_{LO}) + J_1(m_{LO}) e^{j\omega_{LO} t} - J_1(m_{LO}) e^{-j\omega_{LO} t} \\ -J_0(\alpha_1 m_{IF}) e^{j\beta_Y} - jJ_1(\alpha_{IF} m_{IF}) e^{j(\omega_{IF} t + \beta_Y + \theta_{IF})} \\ -jJ_1(\alpha_{IF} m_{IF}) e^{-j(\omega_{IF} t - \beta_Y + \theta_{IF})} \\ +J_2(\alpha_{IF} m_{IF}) e^{j(2\omega_{IF} t + \beta_Y + 2\theta_{IF})} \\ +J_2(\alpha_{IF} m_{IF}) e^{-j(2\omega_{IF} t - \beta_Y + 2\theta_{IF})} \\ +jJ_3(\alpha_{IF} m_{IF}) e^{j(3\omega_{IF} t + \beta_Y + 3\theta_{IF})} \\ +jJ_3(\alpha_{IF} m_{IF}) e^{-j(3\omega_{IF} t - \beta_Y + 3\theta_{IF})} \end{bmatrix} \quad (7)$$

where $\theta_{IF(LO)}$ and $\alpha_{IF(LO)}$ are the phase and amplitude imbalance of the 90° hybrid coupler used to split the IF signal (LO) respectively, and $\beta_{X(Y)}$ is the drift of $\mathrm{DDMZM_{X(Y)}}$ bias angle from the minimum transmission point. Under the ideal situation, $\theta_{IF(LO)} = 0°$, $\alpha_{IF(LO)} = 1$ and $\beta_{X(Y)} = 0°$, (6) and (7) become (2) and (3). The amplitude of the photocurrent at the RF signal frequency, the carrier frequency and the sideband frequency can be obtained from (4), (6) and (7). They are given by

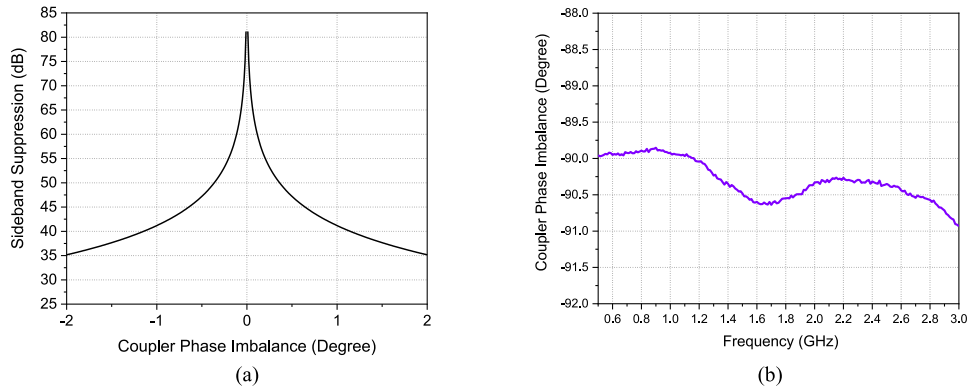

Fig. 3. (a) Simulated SSB mixer sideband suppression versus the phase imbalance of the 90° hybrid coupler that is used to split the IF signal. (b) Measured phase difference between the two outputs of a commercial 0.65-2.8 GHz bandwidth 90° hybrid coupler.

$$I_{f_{LO}+f_{IF}} = \frac{1}{4}\Re P_{in} t_{ff}\Big[\left(J_1\left(m_{LO}\right) J_1\left(\alpha_{IF} m_{IF}\right)\cos(\beta_Y)\right)^2 + \left(J_1\left(\alpha_{LO} m_{LO}\right) J_1\left(m_{IF}\right)\cos(\beta_X)\right)^2 + 2J_1\left(\alpha_{LO} m_{LO}\right) J_1\left(m_{IF}\right) J_1\left(m_{LO}\right) J_1\left(\alpha_{IF} m_{IF}\right)\cos(\beta_X)\cos(\beta_Y)\cos(\theta_{IF}-\theta_{LO})\Big] \quad (8)$$

$$I_{f_{LO}} = \frac{1}{4}\Re P_{in} t_{ff}\Big[\left(J_1\left(\alpha_{LO} m_{LO}\right) J_0\left(m_{IF}\right)\sin(\beta_X)\right)^2 + \left(J_1\left(m_{LO}\right) J_0\left(\alpha_{IF} m_{IF}\right)\sin(\beta_Y)\right)^2 - 2J_1\left(\alpha_{LO} m_{LO}\right) J_0\left(m_{IF}\right) J_1\left(m_{LO}\right) J_0\left(\alpha_{IF} m_{IF}\right)\sin(\beta_X)\sin(\beta_Y)\sin(\theta_{LO})\Big] \quad (9)$$

$$I_{f_{LO}-f_{IF}} = \frac{1}{4}\Re P_{in} t_{ff}\Big[\left(J_1\left(\alpha_{LO} m_{LO}\right) J_1\left(m_{IF}\right)\cos(\beta_X)\right)^2 + \left(J_1\left(m_{LO}\right) J_1\left(\alpha_{IF} m_{IF}\right)\cos(\beta_Y)\right)^2 - 2J_1\left(\alpha_{LO} m_{LO}\right) J_1\left(m_{IF}\right) J_1\left(m_{LO}\right) J_1\left(\alpha_{IF} m_{IF}\right)\cos(\beta_X)\cos(\beta_Y)\cos(\theta_{IF}+\theta_{LO})\Big] \quad (10)$$

III. Simulation Results and Discussion

The effect of the 90° hybrid coupler amplitude and phase imbalance and dual-drive MZM bias angle drift on the RF signal, carrier and sideband power are investigated. Since the LO is a single frequency tone, a variable attenuator and a phase trimmer can be connected to a LO 90° hybrid coupler output to eliminate the amplitude and phase imbalance of the LOs into $\mathrm{DDMZM_X}$ and $\mathrm{DDMZM_Y}$. In contrast, the IF signal has a band of frequency. Sideband suppression, which is defined as the output RF signal to sideband power ratio, was plotted as a function of the IF 90° hybrid coupler phase imbalance and is shown in Fig. 3(a). This shows the phase imbalance of the IF 90° hybrid coupler needs to be less than $\pm 1.1°$ in order to ensure the sideband suppression is above 40 dB. Fortunately, the IF signal is a low-frequency signal and hence a low-frequency 90° hybrid coupler can be used to produce two quadrature-phase IF signals. As shown in Fig. 3(b), a commercial 0.65-2.8 GHz 90° hybrid coupler has less than $\pm 0.7°$ phase imbalance throughout its bandwidth. Fig. 4(a) shows the amplitude imbalance of the IF 90° hybrid coupler needs to be less than ± 0.2 dB in order to obtain above 40 dB sideband suppression. This is a tight requirement but is achievable. This can be seen from the amplitude imbalance of the 0.65-2.8 GHz bandwidth 90° hybrid coupler shown in Fig. 4(b). The figure shows the amplitude difference between the two coupler outputs is less than 0.38 dB in the frequency range of 1.5 to 2.6 GHz. By introducing a fixed 0.57 dB attenuation to the IF 90° hybrid coupler output that has a small insertion loss, less than ± 0.2 dB amplitude imbalance can be obtained over the 1.5 to 2.6 GHz frequency range. Alternatively, it can be seen from (10) that the effect of the amplitude and phase imbalance in the IF 90° hybrid coupler on the sideband photocurrent amplitude can be compensated by introducing an amplitude and phase imbalance to the LOs via a variable attenuator and a phase trimmer.

Modulator bias drift has little effect on the sideband suppression. It mainly affects the amplitude of the carrier at f_{LO}. The proposed SSB mixer enables off-the-shelf bias controllers to be incorporated into the system to eliminate the bias drift problem. This is done by connecting the bias controllers to a built-in PD at the output of each dual-drive MZM inside a commercial DPol-DDMZM (Fujitsu FTM7980EDA). Therefore, changes in the modulator bias point can be monitored by a bias controller, which adjusts the DC voltage into the dual-drive MZM accordingly to lock the modulator at the minimum transmission point. Fig. 5 shows the bias angle needs to be within $\pm 0.26°$ in order to obtain >40 dB carrier suppression. Commercial modulator bias controllers such as Plugtech MBC-MZM-01A ultra high precision MZM bias controller have an offset function that provides accurate control of the modulator bias angle at the null bias mode. This eliminates the modulator bias drift problem so that large carrier suppression can be maintained.

Note that, instead of having an RF signal at f_{LO}+f_{IF}, an RF signal at f_{LO}-f_{IF} can be obtained by introducing a 90° phase shift to the LO into $\mathrm{DDMZM_Y}$ rather than into $\mathrm{DDMZM_X}$ shown in Fig. 1. The performance of the carrier and sideband suppression remain the same as that shown in Fig. 3 to 5. Also note that

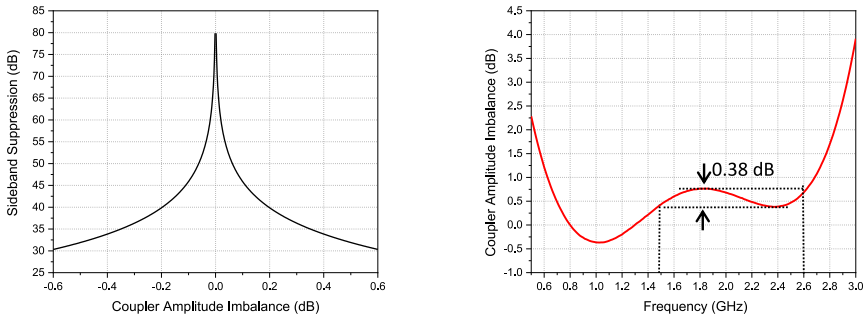

Fig. 4. (a) Simulated SSB mixer sideband suppression versus the amplitude imbalance of the 90° hybrid coupler that is used to split the IF signal. (b) Measured amplitude difference between the two outputs of a commercial 0.65-2.8 GHz bandwidth 90° hybrid coupler.

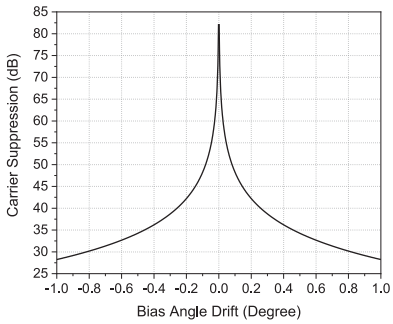

Fig. 5. Simulated carrier suppression versus drift in $DDMZM_X$ bias angle.

no optical filtering is required in the proposed SSB mixer. The RF signal is generated by two sets of LO and IF sidebands beat at the PD. This results in a 6 dB higher conversion efficiency, which is defined as the ratio of the output RF signal power to the input IF signal power, compared to the reported SSB mixer that uses an optical filter to remove either the upper or lower LO sideband [14]. The proposed SSB mixer has a simpler structure compared to the reported SSB mixer that requires path length matching between a polarisation beam splitter and two PDs [13], which is difficult at millimeter wave frequencies. The proposed SSB mixer allows frequency conversion of a low-frequency IF signal into an RF signal at millimeter wave frequencies. On the other hand, the frequency of the output RF signal in the reported structure [12] is limited by the 90° hybrid coupler bandwidth as the 90° hybrid coupler used in the structure needs to split both LO and IF signal. A wide bandwidth 90° hybrid coupler that simultaneously covers an LO at millimeter wave band and a low-frequency IF signal at around 1 GHz does not exist.

IV. Experimental Results

To verify the principle of the proposed SSB mixer, an experiment similar to that shown in Fig. 1 was set up. The laser source was a tunable laser (Keysight N7711A). The continuous wave light generated by the tunable laser had a wavelength of 1550 nm and an optical power of 15.6 dBm. A polarisation controller was connected at the tunable laser output, which was used to ensure the polarisation state of the light is aligned to the slow axis before entering the DPol-DDMZM (Fujitsu FTM7980EDA). The half-wave voltages of the dual-drive MZMs in the DPol-DDMZM were measured to be 3.5 V and 4 V at 1 GHz and 11 GHz respectively. An IF signal generated by a microwave signal generator (Keysight N5173B) was applied to a 0.65-2.8 GHz bandwidth 90° hybrid coupler. The phase and amplitude imbalance between the two coupler outputs were measured on a network analyser and are shown in Fig. 3(b) and 4(b). The 0° and 90° ports of the coupler were connected to one RF port of $DDMZM_X$ and $DDMZM_Y$ respectively. An LO from another microwave signal generator (Analog Devices HMC-T2220) was divided into two via a power divider. One of the power divider outputs was connected to a phase shifter and the other output was connected to a variable attenuator. The phase shifter and the variable attenuator were used to ensure the LO into $DDMZM_X$ and $DDMZM_Y$ have the same amplitude and a 90° phase difference. DC voltages were applied to the DPol-DDMZM to bias both $DDMZM_X$ and $DDMZM_Y$ at the minimum transmission point. An erbium-doped fibre amplifier was connected at the DPol-DDMZM output. This was followed by a 0.5 nm bandwidth tunable optical filter to suppress the amplified spontaneous emission noise. The average optical power into the PD (Discovery Semiconductor DSC30S) was 10 dBm. An electrical signal analyser (ESA) (Keysight N9000A) was connected to the PD output to measure the SSB mixer output electrical spectrum.

The frequency of the IF signal and LO were set at 1 GHz and 11 GHz respectively. The voltage of the IF signal into the DPol-DDMZM was 0.22 V. Hence the IF signal modulation index was 0.2. This enables a high output RF signal to intermodulation product power ratio to be obtained, as was discussed in Section II. The voltage of the LO into the DPol-DDMZM was 0.38 V. Hence the LO modulation index was 0.3. The reason of choosing an LO modulation index of 0.3 is to ensure a high conversion efficiency to be obtained for a fixed average optical power into the photodetector and to minimise changes in the average output optical power when the IF signal modulation index changes [5]. The phase shifter was adjusted to introduce a $+90°$ phase shift to the 11 GHz LO into $DDMZM_X$. Fig. 6(a) shows the measured SSB mixer output electrical spectrum. This shows the RF signal is located at 12 GHz, which is 48.2 dB higher than the carrier at 11 GHz and 50 dB higher than the sideband at 10 GHz. The present of the carrier and sideband are

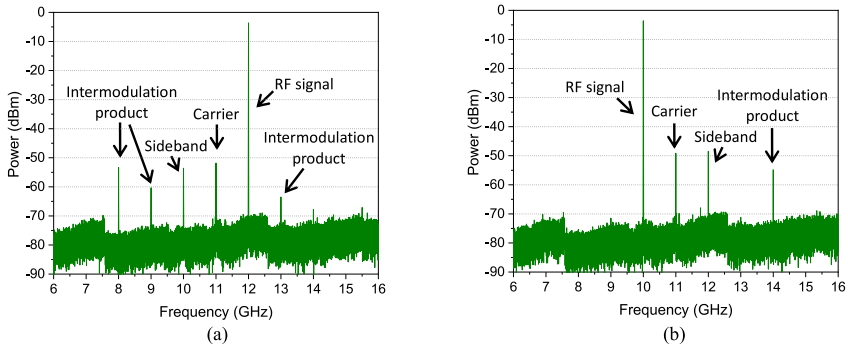

Fig. 6. SSB mixer output electrical spectrum when the 11 GHz LO into $DDMZM_X$ has (a) +90° phase shift and (b) -90° phase shift relative to that into $DDMZM_Y$.

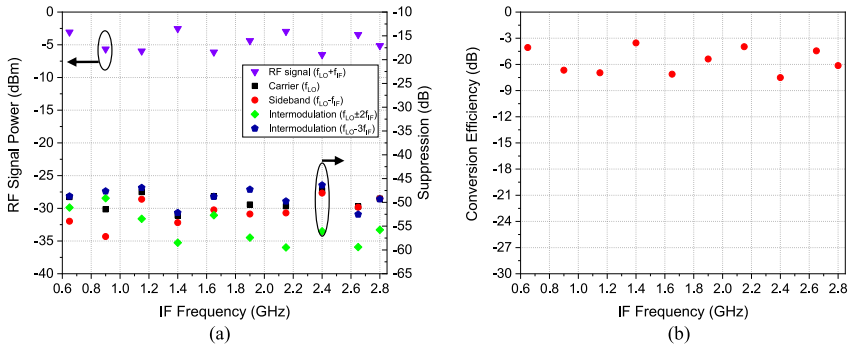

Fig. 7. (a) Measured output RF signal power, and the carrier, sideband and intermodulation suppression for different input IF signal frequencies. (b) The conversion efficiency obtained from the measured output RF signal power.

due to the 90° hybrid coupler amplitude and phase imbalance, and the modulator bias voltages are slightly away from the optimum values. The intermodulation product (f_{LO}-3f_{IF}) at 8 GHz, which is present even under an ideal situation, is 49.8 dB below the RF signal. The phase shifter was then adjusted to introduce a -90° phase shift to the 11 GHz LO into $DDMZM_X$. This changed the RF signal frequency from 12 GHz to 10 GHz as shown in Fig. 6(b). The suppression of the carrier at 11 GHz, the sideband at 12 GHz and the intermodulation product (f_{LO}+3f_{IF}) at 14 GHz are 45.5 dB, 44.9 dB and 51.2 dB respectively. This demonstrates the RF signal can be located at either f_{LO}+f_{IF} or f_{LO}-f_{IF} while having large carrier, sideband and intermodulation suppression.

The performance of the SSB mixer for different IF signal and LO frequencies were investigated. First, the LO frequency was fixed at 11 GHz and the IF signal frequency was varied from 0.65 to 2.8 GHz with a step of 0.25 GHz. Fig. 7(a) shows the measured output RF signal power and the carrier, sideband and intermodulation suppression versus the IF signal frequency. This shows the intermodulation at f_{LO}-3f_{IF} is the highest unwanted frequency component and a high suppression of over 45 dB is obtained throughout the IF signal frequency range of 0.65 to 2.8 GHz. Fig. 7(b) shows the SSB mixer has a high conversion efficiency of around -6 dB. Next, the IF signal frequency was fixed at 1 GHz and the LO frequency was varied. The LO power was adjusted as the LO frequency changed so that the LO modulation index was fixed at 0.3. Fig. 8 shows the SSB mixer output electrical spectrum when the LO frequency is 7 GHz and 18 GHz. This shows the 1 GHz IF signal is upconverted into an 8 GHz and 19 GHz RF signal respectively. More importantly, the carrier, sideband and intermodulation products are more than 44 dB below the output RF signal. The output RF signal power, and the carrier, sideband and intermodulation suppression were measured for every 2 GHz change in the LO frequency from 3 to 18 GHz. Fig. 9(a) shows large suppression of over 45 dB is obtained when the LO frequency is above 7 GHz. Note that, when the LO frequency is 5 GHz, the intermodulation product at f_{LO}-3f_{IF} is located at 2 GHz, which aligns with the second harmonic of the input IF signal. Similarly, when the LO frequency is 3 GHz, the sideband and the intermodulation product at f_{LO}-2f_{IF} are located at 2 GHz and 1 GHz respectively, which align with the second harmonic and the fundamental of the input IF signal. This is the reason why reduction of the sideband and intermodulation product suppression are seen at these LO frequencies. Fig. 9(b) shows there is less than 2.5 dB change in the SSB mixer conversion efficiency as the LO frequency changes from 3 to 18 GHz. The results demonstrate the SSB mixer can be operated over a wide frequency range. Furthermore, both the conversion efficiency and the carrier and sideband suppression are around 10 dB higher than all the reported photonics-based SSB mixers [9]–[14]. The 1-dB compression point of the SSB mixer was also measured. This was done by increasing the input IF signal power until the conversion efficiency reduces by 1 dB from its constant value. It was found to be 12.1 dBm.

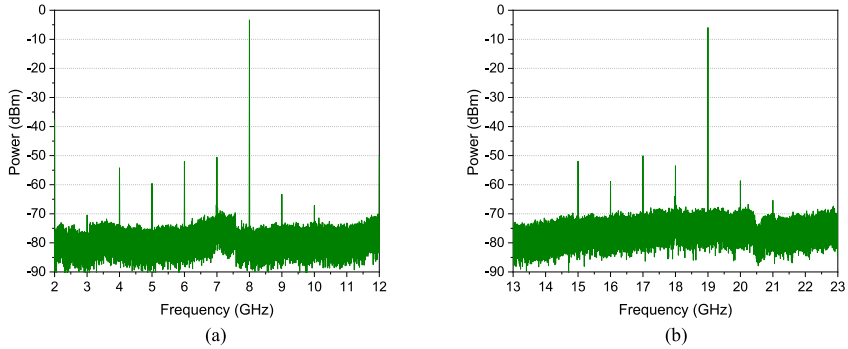

Fig. 8. SSB mixer output electrical spectrum for an LO frequency of (a) 7 GHz and (b) 18 GHz.

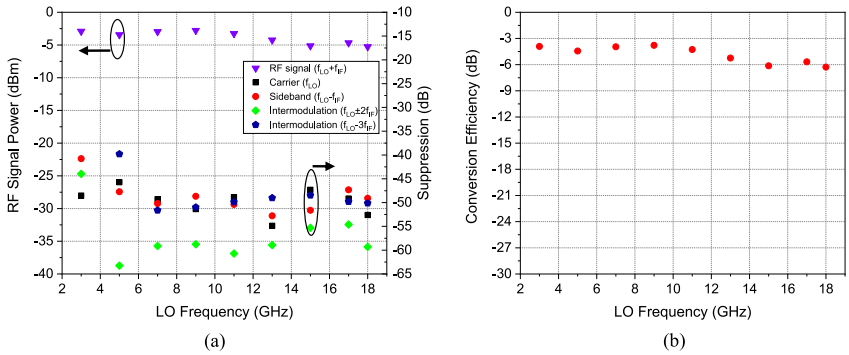

Fig. 9. (a) Measured output RF signal power, and the carrier, sideband and intermodulation suppression for different LO frequencies. (b) The conversion efficiency obtained from the measured output RF signal power.

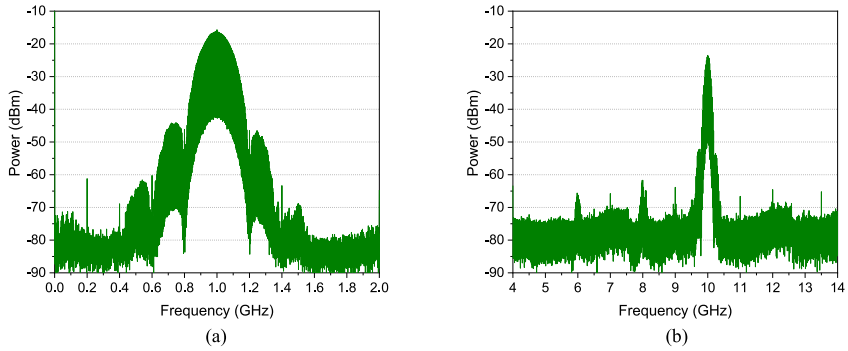

Fig. 10. (a) Measured electrical spectrum of a 200 Mbps PRBS signal at 1 GHz into the SSB mixer and (b) the corresponding SSB mixer output electrical spectrum.

The performance of the proposed SSB mixer was investigated when an IF signal with a band of frequency was applied to the modulator. The IF signal was a 14 dBm 200 Mbps PRBS signal generated by a waveform generator (Keysight 33621A). It was upconverted to 1 GHz via an electronic mixer (Marki T3-06LQP) so that the IF signal was located inside the bandwidth of the 0.65-2.8 GHz 90° hybrid coupler. A 0.4 GHz high pass filter followed by a 1.2 GHz low pass filter were connected after the electronic mixer to suppress the baseband and harmonic components. Fig. 10 shows the electrical spectrum of the 200 Mbps PRBS signal at 1 GHz into the DPol-DDMZM and the SSB mixer output electrical spectrum when a 9 GHz LO into the DPol-DDMZM. The result shows the sideband at 8 GHz is the highest unwanted frequency component. It is 38.2 dB below the upconverted RF signal at 10 GHz. This demonstrates close to 40 dB suppression can be obtained when the IF signal into the SSB mixer has a band of frequency.

As in all reported microwave photonic based SSB mixers, the carrier and sideband suppression of the proposed SSB mixer are affected by the modulator bias drift. Fig. 11(a) shows the SSB mixer output stability measurement when DC power supplies were used to bias $\mathrm{DDMZM_X}$ and $\mathrm{DDMZM_Y}$ inside the DPol-DDMZM at the minimum transmission point. It can be seen from the figure that the carrier power largely increases from -52 dBm to -11.1 dBm in 10 minutes. The sideband power also increases by around 20 dB after 10 minutes. In order to avoid

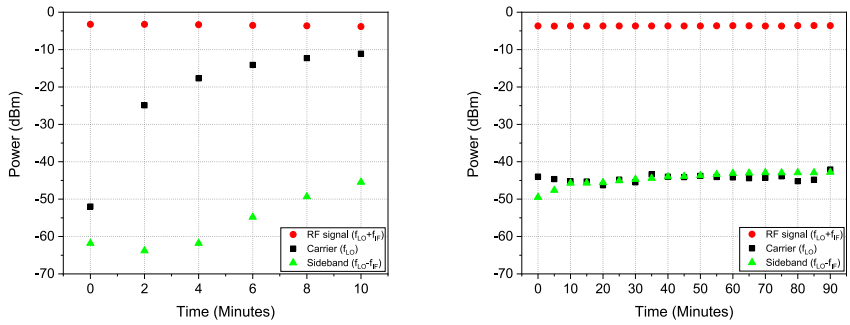

Fig. 11. SSB mixer output stability measurement when (a) DC power supplies and (b) bias controllers are used to bias $\mathrm{DDMZM_X}$ and $\mathrm{DDMZM_Y}$ at the minimum transmission point.

the modulator bias drift problem that degrades the SSB mixer performance, bias controllers (Plugtech MBC-MZM-01A) were used to monitor the two dual-drive MZM bias drifts and to adjust the DC bias voltages accordingly to lock the modulators at the minimum transmission point. As shown in Fig. 11(b), both the carrier and sideband power can be maintained at around −45 dBm over 90 minutes. This demonstrates, for the first time that, a stable long-term large carrier and sideband suppression in a photonics-based SSB mixer. Note that Fig. 11(b) shows the sideband power gradually increases from -49.5 dBm to -42.8 dBm after 90 minutes. This was found to be due to slight changes in the amplitude and phase difference of the two LOs into the DPol-DDMZM. A phase shifter and variable attenuator that provide a fixed phase shift and attenuation over a long period of time, can be used to further improve the stability of the sideband suppression.

V. Conclusion

Microwave photonic offers important advantages for microwave signal frequency conversion. A new photonics-based frequency mixer has been presented which addresses the issue of limited carrier and sideband suppression in the reported SSB mixer structures. It is based on two quadrature-phase LO and IF signals into two parallel-connected dual-drive MZMs. The carrier at f_{LO}, sideband at f_{LO}-f_{IF} and intermodulation products at $f_{LO}\pm 2f_{IF}$ and $f_{LO}\pm 3f_{IF}$ are suppressed after photodetection leaving the up converted RF signal at $f_{LO}+f_{IF}$ at the mixer output. The RF signal frequency can be changed from $f_{LO}+f_{IF}$ to f_{LO}-f_{IF} by changing the LO phase shift from +90° to -90° into a dual-drive MZM inside the DPol-DDMZM. No optical filtering is needed in the proposed mixer structure. The RF signal is generated by beating of two sets of LO and IF signal sidebands at the PD, which results in a high conversion efficiency compared to the reported mixer structures that use an optical filter to remove one sideband. Other advantages of the proposed SSB mixer include long-term stable performance and wide LO and IF signal frequency ranges. Experimental results demonstrate more than 40 dB carrier and sideband suppression and around -6 dB conversion efficiency. Both are over 10 dB higher than the reported photonics-based SSB mixers. Around 40 dB carrier and sideband suppression can be obtained for up converting a 200 Mbps PRBS signal at 1 GHz into an RF signal at 10 GHz. Maintaining around 40 dB carrier and sideband suppression over 90 minutes has been demonstrated for the first time in a photonics-based SSB mixer.

References

[1] X. Xu *et al.*, "Broadband microwave frequency conversion based on an integrated optical micro-comb source," *J. Lightw. Technol.*, vol. 38, no. 2, pp. 332–338, Jan. 2020.
[2] A. C. Lindsay, G. A. Knight, and S. T. Winnall, "Photonic mixers for wide bandwidth RF receiver applications," *IEEE Trans. Microw. Theory Techn.*, vol. 43, no. 9, pp. 2311–2317, Sep. 1995.
[3] H. J. Song, J. S. Lee, and J. I. Song, "Signal up-conversion by using a cross-phase-modulation in all-optical SOA-MZI wavelength converter," *IEEE Photon. Tech. Lett.*, vol. 16, no. 2, pp. 593–595, Feb. 2004.
[4] Y. L. Guennec, G. Maury, J. Yao, and B. Cabon, "New optical microwave up-conversion solution in radio-over-fiber networks for 60-GHz wireless applications," *J. Lightw. Technol.*, vol. 24, no. 3, pp. 1277–1282, Mar. 2006.
[5] E. H. W. Chan and R. A. Minasian, "Microwave photonic downconverter with high conversion efficiency," *J. Lightw. Technol.*, vol. 30, no. 23, pp. 3580–3585, Dec. 2012.
[6] T. Jiang, R. Wu, S. Yu, D. Wang, and W. Gu, "Microwave photonic phase-tunable mixer," *Opt. Exp.*, vol. 25, no. 4, pp. 4519–4527, 2017.
[7] J. Zhang, E. H. W. Chan, X. Wang, X. Feng, and B. Guan, "Broadband microwave photonic sub harmonic downconverter with phase shifting ability," *IEEE Photon. J.*, vol. 9, no. 3, May 2017, Art. no. 5501910.
[8] T. Li, E. H. W. Chan, X. Wang, X. Feng, B. Guan, and J. Yao, "Broadband photonic microwave signal processor with frequency up/down conversion and phase shifting capability," *IEEE Photon. J.*, vol. 10, no. 1, Feb. 2018, Art. no. 5500112.
[9] Q. Guo, E. Xu, and Z. Zhang, "Switchable and filter-free photonic microwave single-sideband frequency converter," *Micro. Opt. Technol. Lett.*, vol. 63, no. 4, pp. 1073–1077, 2021.
[10] Y. Gao, A. Wen, W. Jiang, Y. Fan, D. Zhou, and Y. He, "Wideband photonic microwave SSB up-converter and I/Q modulator," *J. Lightw. Technol.*, vol. 35, no. 18, pp. 4023–4032, Sep. 2017.
[11] Y. Gao, A. Wen, W. Jiang, Y. Fan, Y. He, and D. Zhou, "Fundamental/subharmonic photonic microwave I/Q up-converter for single sideband and vector signal generation," *IEEE Trans. Microw. Theory Techn.*, vol. 66, no. 9, pp. 4282–4292, Sep. 2018.
[12] Z. Tang and S. Pan, "A filter-free photonic microwave single sideband mixer," *IEEE Microw. Wireless Compon. Lett.*, vol. 26, no. 1, pp. 67–69, Jan. 2016.
[13] Z. Tang and S. Pan, "A compact image-reject and single-sideband mixer with suppression of LO leakage based on a dual-polarization dual-drive mach-zehnder modulator," in *Proc. IEEE Int. Topical Meeting Microw. Photon.*, 2016, pp. 79–82.
[14] C. Huang, E. H. W. Chan, and C. B. Albert, "A compact photonics-based single sideband mixer without using high-frequency electrical components," *IEEE Photon. J.*, vol. 11, no. 4, Aug. 2019, Art. no. 7204509.